Chemical Geology 383 (2014) 100–106

Contents lists available at ScienceDirect

Chemical Geology

journal homepage: www.elsevier.com/locate/chemgeo

Redox-driven dissolution of clay minerals by uranium under high pressure CO_2 conditions

Yan Liu, Fubo Luan, William D. Burgos *

Department of Civil and Environmental Engineering, The Pennsylvania State University, University Park, PA 16801-1408, United States

ARTICLE INFO

Article history:
Received 18 December 2013
Received in revised form 9 June 2014
Accepted 12 June 2014
Available online 21 June 2014

Editor: J. Fein

Keywords:
Carbon sequestration
Iron-bearing clay minerals
Uranium

ABSTRACT

Geologic sequestration of supercritical CO_2 is one technology proposed to mitigate global warming. Increased acidity of brine due to CO_2 injection could lead to mineral dissolution of cap rock and well seals and mobilization of contaminants (e.g., U, Pb, As). In this study we examined the dissolution of nontronite NAu-2, an Fe(III)-rich clay mineral, and partially-reduced nontronite (R-NAu-2) in a synthetic brine (0.33 M Na_2SO_4) under high pressure CO_2 conditions (P_T = 9.66 bar, $P_{CO_2} \geq$ 8.66 bar CO_2, T = 20 °C) and in 1.40 M H_3PO_4–0.50 M H_2SO_4. Uranyl(VI) or biogenic uraninite(IV) was added as a redox-active contaminant and reaction kinetics were measured over a 15 d period. Unaltered nontronite [3.4% Fe(II)] dissolved very little under high pressure CO_2 conditions. However, chemically-reduced nontronite [48% Fe(II)] dissolved more rapidly (half-life of 78.4 d under high pressure CO_2 conditions, 17.8 h in H_3PO_4–H_2SO_4). Structural Fe(II) in reduced nontronite [R-NAu-2 Fe(II)] was preferentially dissolved compared to structural Fe(III) in unaltered nontronite [NAu-2 Fe(III)]. No redox reactions were observed between R-NAu-2 Fe(II) and U(VI). In contrast, uraninite was oxidized by NAu-2 Fe(III) faster and to a greater extent under high pressure CO_2 conditions as compared to ambient pressure conditions (P_T = 1.0 bar, 95:5% N_2:H_2). Redox reactions between uraninite and NAu-2 Fe(III) enhanced the dissolution of both clay and U, indicative of potential risks associated with geologic carbon sequestration.

1. Introduction

Geologic carbon sequestration (GCS) is a process where CO_2 is captured, transported and injected into underground reservoirs such as saline aquifers, depleted oil and gas reservoirs, and un-mineable coal seams. The advantage of saline aquifers is their wide distribution and large capacity. It was estimated that 65% of CO_2 produced by power plants in the United States can be injected directly into deep saline aquifers below the plants (White et al., 2005). The introduction of CO_2 into saline aquifers will decrease the pH of the brine, especially if impurity gases such as NO_x and SO_x are present (Knauss et al., 2005; Xu et al., 2007). For example, Knauss et al. modeled geochemical changes in the saline Frio Formation caused by CO_2 injection with and without trace impurities. They reported that the lowest pH values adjacent to the injection well would be pH 3.2 at an injection pressure of 84.3 bar CO_2 but this would decrease to pH 1.0 with the addition of 10^{-6} bar of SO_2 (Knauss et al., 2005).

Decreased pH and increased dissolved carbonate concentrations will induce dissolution and precipitation of minerals in the storage reservoir. Mineral trapping of CO_2 into e.g. carbonate minerals would promote CO_2 sequestration but possibly decrease reservoir porosity. A number of experimental studies have taken intact cores from reservoir formations, flooded these cores with CO_2-rich fluids and measured increases in porosity and permeability (Rimmele et al., 2010; Canal et al., 2013). Other studies have reported that porosity and permeability of Stuttgart sandstone (Sell et al., 2013), Glauconitic sandstone, Gulf Coast sediments and dunite (Xu et al., 2004) decreased after reaction with CO_2-rich fluids.

Clays and clay minerals are ubiquitous in sedimentary rocks, especially shale. More than 60% of depleted petroleum reservoirs are capped by shale (Olabode et al., 2012). Clay minerals such as bentonite are also an important component of cement used in wellbore seals for geologic carbon sequestration. While clays are generally considered as refractory materials that are difficult to dissolve, low-pH conditions and long-term exposure within storage reservoirs may promote dissolution. Shaw and Hendry (2009) developed a conceptual model for acid-promoted dissolution of clay minerals. At pH > 3, tetrahedral and octahedral sheets are not dissolved but exchangeable cations in the interlayers are replaced by H^+. At 3 > pH > 1, octahedral sheets begin to dissolve before tetrahedral sheets. At pH < 1, tetrahedral sheets begin to dissolve. Clay minerals dissolve in strong acid, such as >1 M H_2SO_4 or HCl, under high temperature (70 to 95 °C) for several hours (Okada et al., 2006; Steudel et al., 2009). In addition to acid-promoted dissolution, Fe(III)-rich clay minerals are subject to redox-promoted dissolution. Reduction of structural Fe(III) has been shown to promote

* Corresponding author at: Dept. of Civil and Environmental Engineering, The Pennsylvania State University, 212 Sackett Building, University Park, PA 16802, United States. Tel.: +1 814 863 0578; fax: +1 814 863 7304.
E-mail address: wdb3@psu.edu (W.D. Burgos).

http://dx.doi.org/10.1016/j.chemgeo.2014.06.009
0009-2541/

clay dissolution (Stucki, 2011; Jaisi et al., 2008). Using infrared spectroscopy (Neumann et al., 2008) and Mössbauer spectroscopy (Ribeiro et al., 2009), irreversible reduction and/or reductive dissolution of structural Fe has been shown to permanently alter the clay structure.

Clay minerals have been identified as key mineral phases affecting the fate and transport of contaminants potentially mobilized by CO_2 sequestration (IEAGHG, 2013). Clay minerals are expected to be important in low hydraulic conductivity zones such as the overlying cap rock and within engineered well seals. The mineralogy of sixteen candidate GCS sites from seven basins within the US DOE Regional Carbon Sequestration Partnership programs were examined and clay minerals were identified as dominant mineral components in eleven of the sixteen sites — illite in eight, glauconite in five, chlorite in four, montmorillonite in four, and smectite in one (Griffith et al., 2011). It is reasonable to assume that some amount of structural iron exists within these clay minerals. We have constructed model systems using specimen clay minerals and U to measure redox dynamics and mineral dissolution under conditions with elevated concentrations of CO_2. Concentrations of clay minerals and U were selected to promote electron transfer reactions between these components and not selected to match in situ concentrations expected at CO_2 sequestration sites.

The US DOE National Energy Technology Laboratory (NETL) and the International Energy Agency (IEAGHG, 2013) have identified U as a contaminant of concern at sites proposed for GCS. While U may not be a common contaminant of concern in CO_2 sequestration strata, the mobilization of U caused by CO_2 leakage and reaction in overlying aquifers is of concern (Keating et al., 2010; Little and Jackson, 2010). One study examined the mobilization of trace contaminants from seventeen freshwater aquifers that overly candidate deep saline GCS sites. When these aquifer sediments were exposed to elevated concentrations of CO_2, dissolved concentrations of U were found to more than double in ten of the seventeen sediments tested (Little and Jackson, 2010). Elevated concentrations of dissolved U were also reported at Chimayó, NM, where CO_2 from natural sources upwells from a deep saline aquifer (Keating et al., 2010). This sedimentary basin has been described as a natural analog site for CO_2 sequestration. Aquifer sediments contain illite and smectite and the brackish, CO_2-rich water was enriched with both Fe and U. Model simulations (Zheng et al., 2009), laboratory experiments (Little and Jackson, 2010), and field site monitoring (Kharaka et al., 2010) have also shown increases in concentrations of As and Pb after injection of CO_2.

The purpose of this research was to investigate dissolution of nontronite, uraninite and redox reactions between them under high pressure CO_2 conditions. Partially-reduced nontronite was used to study the influence of Fe(II/III) speciation on nontronite dissolution and its redox reactions with U(VI). A stronger acid, 1.40 M H_3PO_4–0.50 M H_2SO_4, was also used to simulate more acidic conditions caused by the possible co-injection of NO_x and SO_x.

2. Materials and methods

2.1. Clay mineral preparation

Nontronite NAu-2, an iron-rich variety of smectite from the Uley graphite mine, South Australia (Keeling et al., 2000), was purchased from the Clay Mineral Society (West Lafayette, IN). Bishop et al. (2011) reported a solid-phase mineral composition of NAu-2 to be $[Ca_{0.28}Na_{4.56}K_{0.42}]_{0.72}(Al_{0.23}Fe^{2+}_{0.06}Fe^{3+}_{3.76}Mg_{0.10}Ti_{0.06})(Si_{7.19}Al_{0.81}Fe_{0.33})O_{20}(OH)_4$. The chemical composition of NAu-2 used in this study will likely vary from this formula due to subtleties between batches and size fractionation techniques. NAu-2 was suspended in 0.1 M NaCl for 24 h and then separated by centrifugation to obtain the 0.5–2.0 μm clay-size fraction. The clay fraction was washed with distilled deionized water (Milli-Q) repeatedly until no Cl^- was detected by silver nitrate and then dried at 80 °C. The NAu-2 clay fraction contained 4.46 mmol Fe/g clay and was 96.6% Fe(III) based on an anoxic HF–H_2SO_4 digestion method (Luan and Burgos, 2012).

NAu-2 stock solutions were prepared at 0.5 g/L in anoxic 0.33 M Na_2SO_4 for high pressure CO_2 dissolution experiments and 1.0 g/L in anoxic 0.66 M Na_2SO_4 for other experiments. Chloride is usually the dominant anion in brines from deep saline aquifers selected for GCS. However, we used a sulfate-brine to avoid analytical interferences with our U(VI) method — a Kinetic Phosphorescence Analyzer (KPA). Chloride will complex with the uranyl cation (UO_2^{2+}) and effectively quench the kinetic phosphorescence reaction. Sulfate is typically the next most abundant anion in saline brines, but often one to two orders of magnitude lower in concentration as compared to chloride (Emberley et al., 2004; Daneshfar et al., 2009).

Partially-reduced nontronite (R-NAu-2) was produced using the citrate–bicarbonate–dithionite (CBD) method (Stucki et al., 1984). Reaction conditions were controlled such that 48% of the structural Fe(III) was reduced. R-NAu-2 was sequentially washed with anoxic 0.1 M NaCl, 0.01 M NaCl, 0.001 M NaCl and three times with anoxic Milli-Q water. R-NAu-2 [48% Fe(II)] stock solutions were prepared at 0.5 g/L in anoxic 0.33 M Na_2SO_4 for high pressure CO_2 dissolution experiments and 1.0 g/L in anoxic 0.66 M Na_2SO_4 for other experiments. All clay mineral stock solutions were stored in flasks sealed by parafilm in an anoxic chamber (supplied with 95:5% N_2:H_2 gas mix).

2.2. Uranium suspensions

Uranyl acetate dihydrate was dissolved in anoxic 30 mM $NaHCO_3$ (pH 6.8) under a 100% N_2 atm to prepare a 0.90 mM U(VI) stock solution. Biogenic uraninite precipitates were produced with *Shewanella putrefaciens* CN32 ($0.5–1.0 * 10^8$ cells/mL; harvested at late-log phase) using uranyl acetate (1.0 mM) as the sole electron acceptor and sodium lactate (5 mM) as the electron donor in anoxic 30 mM $NaHCO_3$ buffer. All methods have been previously described (Senko et al., 2007; Burgos et al., 2008). After a three month incubation period, the cell-uraninite suspension was transferred into O_2-free, anoxic 10% NaOH and mixed for two days to digest cell material, washed three times with anoxic 24 mM $NaHCO_3$ and twice with anoxic Milli-Q water (Ginder-Vogel et al., 2006). The uraninite precipitates contained 58% U(IV) based on an H_3PO_4–H_2SO_4 extraction and automated anoxic KPA method (Luan and Burgos, 2012). The relatively high proportion of U(VI) was likely caused by centrifugation performed outside of the anoxic chamber. Ulrich et al. (2009) also reported that treatment of biogenic uraninite with 1 M NaOH led to partial oxidation of the uraninite. At high pH conditions, water radiolysis products could serve as oxidants in otherwise anoxic water.

2.3. Clay dissolution experiments

High pressure CO_2 conditions were established by adding 0.8 g dry ice (Kelly Dry Ice Co. Inc., food grade) to 38 mL pressure tubes (Ace Glass, Inc., Model 8648) containing 10 mL 0.5 g/L clay minerals in 0.33 M Na_2SO_4 brine. Pressure tubes were washed with 10–15% nitric acid and rinsed with Milli-Q water before use. All reactor preparation before adding dry ice was done inside an anoxic chamber (supplied with 95:5% N_2:H_2 gas mix). Due to operational difficulties of moving dry ice through an interlock chamber and into an anoxic chamber, pressure tubes were opened under ambient atmospheric conditions. Tubes were opened, dry ice added, and capped within 10 s. Dry ice added to the brine immediately created CO_2 gas in the tube. With an initial atmosphere of 1 bar 95:5% N_2:H_2 and immediate CO_2 degassing, we assumed that little to no oxygen entered the pressure tube during dry ice addition. After capping the tube, the pressure reached 9.66 bar within 10 min (measured with pressure gauge attached within seal plug). After 15 d, the tube pressure had relaxed to ca. 7.17 bar. All pressure tubes were mixed at 100 rpm in a 20 °C constant-temperature room. Control reactors with dry ice but no clay mineral or no dry ice with

clay mineral (prepared and maintained under $P_T = 1.0$ bar, 95:5% N_2:H_2) were also established. Based on these operational methods, we have adopted the following terminology to describe our reactors. "High pressure CO_2 conditions" refer to $P_T = 9.66$ bar with $P_{CO_2} \geq 8.66$ bar (initially). "Ambient pressure conditions" refer to $P_T = 1.0$ bar, 95:5% N_2:H_2. Reaction kinetics were measured over a 15 d period by sacrificing pressure tubes.

Clay minerals were also dissolved in 1.40 M H_3PO_4–0.50 M H_2SO_4 under ambient pressure conditions using 0.5 g/L clay in 0.33 M Na_2SO_4 brine mixed in flasks inside an anoxic chamber. No-clay control reactors were prepared with all experiments. The combination and concentrations of H_3PO_4–H_2SO_4 were based on a previous analytical method developed for clay-Fe(II/III) and U(IV/VI) speciation (Luan and Burgos, 2012). Reaction kinetics were measured over a 3 d period.

2.4. Clay–uranium experiments

Clay–uranium experiments were initiated by mixing 1.0 g/L NAu-2 or R-NAu-2 in 0.66 M Na_2SO_4 brine with U(VI) (in 30 mM $NaHCO_3$) or uraninite (in Milli-Q water) stock solution at a 1:1 volume ratio. Final concentrations in the pressure tubes were 0.5 g/L NAu-2 or R-NAu-2, 0.33 M Na_2SO_4, with 15 mM $NaHCO_3$ and 0.45 mM U(VI) for U(VI) experiments, or with 0.33 mM uraninite [58% U(IV)] for U(IV) experiments. Total suspension volume in each pressure tube was approximately 10 mL. Experiments were conducted under both high pressure CO_2 conditions and ambient pressure conditions. Control reactors with U but no-clay were prepared with all experiments. Control reactors with clay and U were also prepared under ambient pressure conditions.

2.5. Analytical methods

In no-uranium reaction systems, the modified HF–H_2SO_4-phenanthroline digestion method was used to measure clay-Fe(II/III) speciation (Luan and Burgos, 2012). In clay–uranium reaction systems, clay-Fe(II/III) was measured using a sequential acid extraction/mineral digestion method (Luan and Burgos, 2012; Figure S1). H_3PO_4–H_2SO_4-extractable Fe(II/III) was measured after the mineral pellet had been extracted for 10 min in 1.40 M H_3PO_4–0.50 M H_2SO_4. HF–H_2SO_4-digestable Fe(II/III) was measured using the remaining mineral pellet following the HF–H_2SO_4-phenanthroline method. Uranium (IV/VI) was measured in the dissolved and H_3PO_4–H_2SO_4-extractable fractions using an anoxic automated KPA method. Dissolved samples were collected after centrifugation (14,000 rpm for 10 min) and before H_3PO_4–H_2SO_4-extraction. U(IV/VI) was speciated by analyzing samples and then re-analyzing samples after they were oxidized with 70% HNO_3 and heated in a boiling water bath for 45 min. Dissolved Fe(II/III) was measured in the supernatant using the phenanthroline method.

Well mixed sample suspensions were filtered (0.2 μm), acidified with 70% nitric acid, and stored at 4 °C until analysis of dissolved cations. Al, Fe, Mg and Si were measured by Inductively Coupled Plasma-Atomic Emission Spectrometry (ICP-AES).

3. Results and discussion

3.1. Dissolution of nontronite NAu-2 and reduced NAu-2

Nontronite did not dissolve to any great extent under high pressure CO_2 conditions ($P_T = 9.66$ bar, $P_{CO_2} \geq 8.66$ bar CO_2, T = 20 °C) during a 15 d reaction period. No differences were found in experiments conducted in 1.0 M NaCl, 0.33 M $CaCl_2$ or 0.33 M Na_2SO_4 (data not shown). There was no more than a sum total of 5 mg/L of dissolved cations (Al, Fe, Mg and Si) detected in these experiments, which accounted for less than 1.1% (converted to oxides) of the total clay mass. Dissolved cation concentrations were calculated from the concentrations measured in the clay-containing pressure tube minus the concentrations measured in the corresponding no-clay control (Table S1). After 1 to 15 d of reaction under high pressure CO_2 conditions, pH values of 10 g/L nontronite suspensions in 1 M $CaCl_2$ ranged from pH 3.98 to 4.15. The limited dissolution of nontronite under these conditions is consistent with the conceptual model for clay dissolution proposed by Shaw and Hendry (2009) where aluminosilicates will not dissolve until pH <3.

In comparison, reduced NAu-2 (48% clay-Fe(II)) dissolved to a quantifiable extent under high pressure CO_2 conditions (Fig. 1a). Based on the sum of dissolved Al, Fe, Mg and Si concentrations measured at the end of the 15 d reaction period, 21% of the total mass of reduced NAu-2 dissolved under high pressure CO_2 conditions. Reduction of

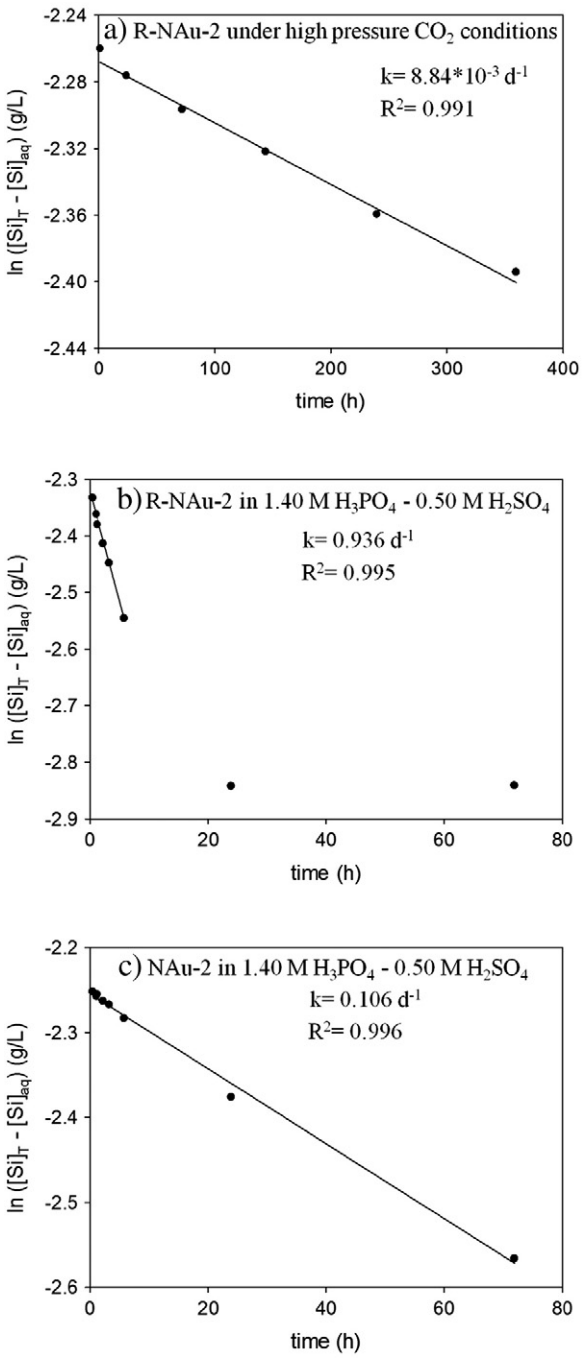

Fig. 1. First order model of dissolution kinetics of Si from: a) 0.5 g/L reduced nontronite NAu-2 in 0.33 M Na_2SO_4 under high pressure CO_2 conditions ($P_T = 9.66$ bar, $P_{CO_2} \geq 8.66$ bar CO_2); b) 0.5 g/L reduced NAu-2 in 0.33 M Na_2SO_4 extracted with 1.40 M H_3PO_4–0.50 M H_2SO_4; and, c) 0.5 g/L NAu-2 in 0.33 M Na_2SO_4 extracted with 1.40 M H_3PO_4–0.50 M H_2SO_4. $[Si]_T$ and $[Si]_{aq}$ represent total Si in clay suspension and dissolved Si, respectively.

structural Fe(III) in nontronite [referred to as NAu-2 Fe(III)] to structural Fe(II) in nontronite [referred to as R-NAu-2 Fe(II)] will result in a charge imbalance (caused by Fe^{3+} converted to Fe^{2+}) that must be compensated within the clay mineral structure and/or through exchange of adsorbed ions. Charge compensation decreased the stability of R-NAu-2 Fe(II) compared to NAu-2 Fe(III) and led to a greater rate and extent of clay mineral dissolution. Previous studies have shown that the substitution of Fe^{2+} or Mg^{2+} for Al^{3+} in the octahedral sheet, or the substitution of Al^{3+} or Fe^{3+} for Si^{4+} in the tetrahedral sheet increased the solubility of illite and smectite in H_2SO_4 or HCl (Steudel et al., 2009; Pentrak et al., 2010).

The dissolution of Si from nontronite was modeled using a pseudo-first order reaction according to:

$$d[Si]_{aq}/dt = -k\left([Si]_T - [Si]_{aq}\right) \quad 1$$

where k is the first order dissolution rate constant (h^{-1}), $[Si]_T$ is the initial total concentration of Si in suspension (g/L), and $[Si]_{aq}$ is the dissolved concentration of Si (g/L) evolving over time. A pseudo-first order reaction has also been used to model the dissolution of Al and Si from montmorillonite and nontronite in acid solutions (Osthaus, 1955; Zysset and Schindler, 1996; Rozalen et al., 2008). An integrated form of Eq. 1 was used to calculate k according to:

$$\ln\left([Si]_T - [Si]_{aq}\right) = -k \times t + b \quad 2$$

where b is an intercept value. The half-life of dissolution was calculated as ln(2)/k. As noted above, the dissolution of nontronite under high pressure CO_2 conditions produced dissolved concentrations of Al, Fe, Mg and Si too low to calculate a statistically meaningful rate constant. The dissolution of Si from R-NAu-2, however, fit well to Eq. 2, with a half-life from 1660 to 2160 h (95% confidence interval, *t*-test, n = 6). As discussed below, while nontronite dissolution was not congruent, kinetic constants for the different clays under the different conditions were still valuable for comparison purposes.

The strong acid 1.40 M H_3PO_4–0.50 M H_2SO_4 significantly increased the rate and extent of dissolution of both nontronite (Fig. 1c) and R-NAu-2 (Fig. 1b). Based on dissolved Al, Fe, Mg and Si concentrations measured at the end of the 3 d reaction period, 23% of the total mass of nontronite dissolved while 70% of the R-NAu-2 dissolved. Dissolution of Si from both nontronites was well fitted by Eq. 2. A half-life from 147 to 168 h (n = 8) was calculated for nontronite in H_3PO_4–H_2SO_4 as compared to a half-life from 16.2 to 19.7 h (n = 6) for R-NAu-2 in H_3PO_4–H_2SO_4. All structural layers of phyllosilicates are expected to dissolve under these extreme acidic conditions (Shaw and Henry, 2009).

Dissolution of nontronite and R-NAu-2 in H_3PO_4–H_2SO_4 was incongruent (Fig. 2). Molar ratios of dissolved Fe to dissolved Al (Fe/Al), Fe/Si, Al/Si and Mg/Al were all essentially greater than the stoichiometric ratios reported previously (Bishop et al., 2011). As noted above, these differences likely reflect some variability in purchased materials and differences caused by our size fractionation procedures. Differences in the absolute values of these molar ratios between nontronite and R-NAu-2 were caused by the CBD reduction procedure (and clay washing) used to produce R-NAu-2. Near-constant Fe/Al ratios for both nontronite and R-NAu-2 (Fig. 2a) suggest that Fe and Al may congruently dissolve out of the octahedral layer of these nontronites. Declining Fe/Si ratios for both nontronite and R-NAu-2 (Fig. 2b) demonstrate that Fe was preferentially dissolved as compared to Si. Conceptually, Fe can be dissolved from the Si-rich tetrahedral layer (presumably accounting for ca. 8% of the total structural clay-Fe) or the Al-rich octahedral layer (92% of structural clay-Fe) (Gates et al.,

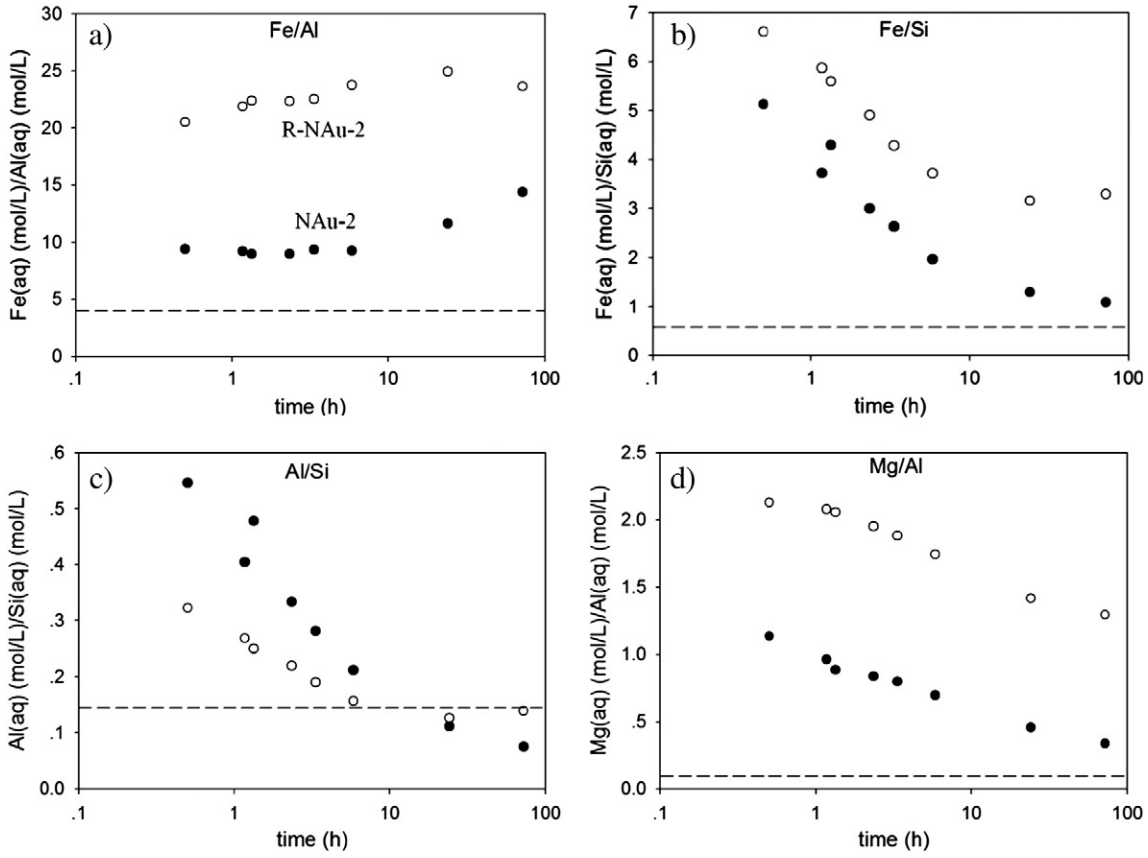

Fig. 2. Ratios of dissolved: a) Fe/Al, b) Fe/Si, c) Al/Si, and d) Mg/Al ((mol/L)/(mol/L)) from nontronite NAu-2 and reduced nontronite R-NAu-2 (both 0.5 g/L) in 0.33 M Na_2SO_4 under ambient pressure conditions (P_T = 1.0, N_2:H_2 = 95:5%) in 1.40 M H_3PO_4–0.50 M H_2SO_4. Dashed lines represent theoretical elemental ratios in unaltered clay mineral.

2002; Jaisi et al., 2005). Octahedral layers dissolve more easily than tetrahedral layers (Shaw and Henry, 2009), suggesting that most of the dissolved Fe originated from octahedral layers. Charge compensation caused by isomorphic substitution of Al^{3+} for Si^{4+} in the tetrahedral layer and isomorphic substitution of Mg^{2+} for Al^{3+} in the octahedral layer can be used to explain the declining Al/Si and Mg/Al ratios, respectively, observed in these experiments (Fig. 2c,d). Overall, preferential dissolution occurred as: Mg > Fe ≈ Al > Si, consistent with several previous studies (Rozalen et al., 2008; Steudel et al., 2009; Pentrak et al., 2010).

3.2. Reactions between nontronite and uranium(VI)

Experiments were conducted with nontronite and uranium to determine if reactions between NAu-2 Fe(III) and U(IV), or R-NAu-2 Fe(II) and U(VI) would promote clay dissolution or uranium solubilization. To accurately speciate both clay-Fe(II/III) and U(IV/VI) in suspensions containing both elements, a sequential acid extraction–mineral digestion procedure was required (H_3PO_4–H_2SO_4 extraction–HF–H_2SO_4-phenanthroline digestion) (Luan and Burgos, 2012). This additional acid extraction step led to the operational measurements of dissolved, H_3PO_4–H_2SO_4-extractable and HF–H_2SO_4-digestable concentrations. Fe(II/III) were speciated in all three fractions while U(IV/VI) were speciated only in the dissolved and H_3PO_4–H_2SO_4-extractable fractions (because H_3PO_4–H_2SO_4 solubilized all U).

As expected, no redox reactions occurred between NAu-2 Fe(III) and U(VI) (Figure S2). U(VI) also did not participate in any redox reactions with R-NAu-2 Fe(II) (Figure S2). Fe(II) was the predominant form of dissolved Fe and the predominant form of H_3PO_4–H_2SO_4-extractable Fe. The preferential solubilization and acid extraction of Fe(II) were expected based on our results with R-NAu-2 in the absence of U. High pressure CO_2 conditions as compared to ambient pressure conditions had no effect on this result. R-NAu-2 Fe(II) was either not a strong enough reductant to reduce U(VI) or it was kinetically limited in its ability to transfer electrons to U(VI). These results are consistent with Zhang et al. (2009) who found that chemically reduced NAu-2 (27% clay-Fe(II), 20 mM clay-Fe) did not react with 1.0 mM U(VI) in a 30 mM $NaHCO_3$ background electrolyte over an 83 d reaction period.

While U(VI) did not participate in redox reactions with R-NAu-2 Fe(II), U(VI) did affect the dissolution of Al, Fe, Mg and Si (Figure S3). The dissolution of Al, Fe and Mg from R-NAu-2 under high pressure CO_2 conditions decreased compared to identical experimental conditions without U, while the dissolution of Si increased slightly. We speculate that the sorption of U(VI) to edge sites of R-NAu-2 may have blocked protons from accessing these sites and re-directed proton attack towards the Si-rich basal planes.

3.3. Reactions between nontronite and uranium(IV)

NAu-2 Fe(III) was reduced and uraninite(IV) was oxidized under both high pressure CO_2 conditions and ambient pressure conditions (Fig. 3). The extent of redox reactions between U(IV) and Fe(III) was greater under high pressure CO_2 conditions. After 360 h, the overall $Fe(II)/Fe_{TOT}$ ratio in nontronite increased from 3.4% to 18.1% under high pressure CO_2 conditions as compared to increasing to 10.5% under ambient pressure conditions (Fig. 3a). The ratio of measured concentrations of Fe(II) produced to U(VI) produced [ΔFe(II)/ΔU(VI)] was close to the theoretical ratio of 2 mol Fe(II) per 1 mol U(VI) (Fig. 4). Lower pH values and higher bicarbonate concentrations under the high pressure CO_2 conditions are expected to increase the rate of uraninite oxidation (Ginder-Vogel et al., 2006) and the thermodynamic driving force for uraninite oxidation coupled to Fe(III) reduction (Ginder-Vogel et al., 2010).

Concentrations of uranium in brine were significantly higher under high pressure CO_2 conditions as compared to ambient pressure conditions (Fig. 4 and Figure S4), which was caused by acid-driven and oxidation-driven dissolution. This is similar to in situ recovery mining of uranium, where oxidizing reagents such as O_2 and H_2O_2, together with CO_2, are pumped with water into a confined aquifer with permeable uranium ore (Borch et al., 2012). Oxidation-driven, acid-driven and bicarbonate-driven dissolution of uraninite enriches U in the recovered water. If geological carbon sequestration takes place in aquifers with uranium and Fe(III)-bearing clay minerals, mobilization of U could occur.

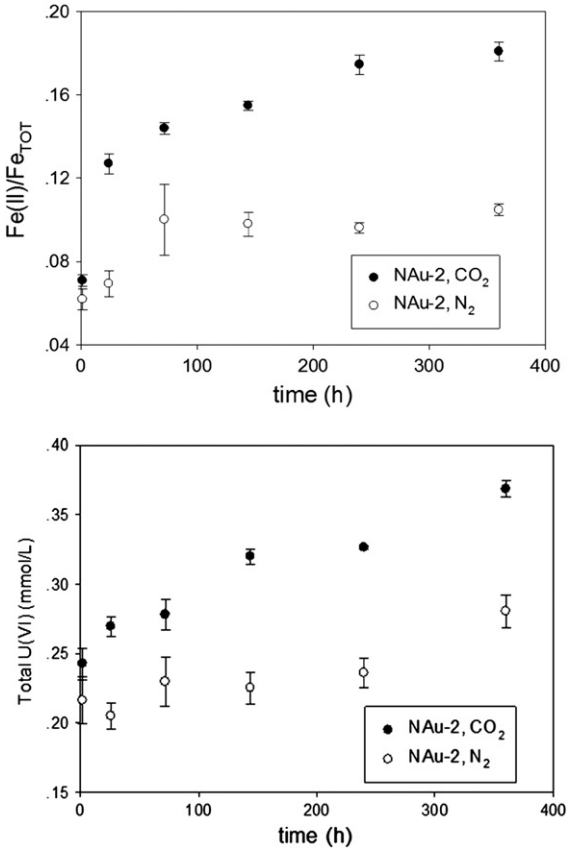

Fig. 3. Reduction kinetics of nontronite NAu-2 by uraninite. a) $Fe(II)/Fe_{TOT}$ ratios in NAu-2, and b) total U(VI) concentrations (sum of dissolved U(VI) and 1.40 M H_3PO_4–0.50 M H_2SO_4 extractable U(VI)). Experiments conducted with 0.5 g/L NAu-2, 0.33 mM uraninite (58% U(IV) at t = 0) in 0.33 M Na_2SO_4 brine under high pressure CO_2 conditions (P_T = 9.66 bar, $P_{CO_2} \geq$ 8.66 bar CO_2) and ambient pressure conditions (P_T = 1.0 bar, N_2:H_2 = 95:5%).

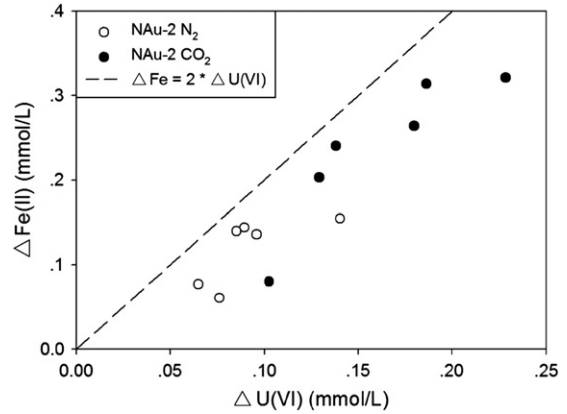

Fig. 4. Stoichiometric relationships between Δ mol Fe(II) and Δ mol U(VI) for the nontronite–uraninite experiments proposed sequential extraction procedure. Experiments conducted with 0.5 g/L NAu-2, 0.33 mM uraninite (58% U(IV)) in 0.33 M Na_2SO_4 brine: (●) under high pressure CO_2 conditions (P_T = 9.66 bar, $P_{CO_2} \geq$ 8.66 bar CO_2), or (○) ambient pressure conditions (P_T = 1.0 bar, N_2:H_2 = 95:5%). Dashed line represents theoretical stoichiometry of 2 Δ mol Fe(II) to 1 Δ mol U(VI).

Uraninite-driven reduction of NAu-2 Fe(III) led to reductive dissolution of the clay mineral only under high pressure CO_2 conditions (Fig. 5). Redox-promoted dissolution of nontronite was consistent with the enhanced solubility of R-NAu-2 as compared to nontronite. Under ambient pressure conditions, concentrations of dissolved Fe were not measureable (1.1 μM detection limit by the phenanthroline method) even after nontronite was reduced by uraninite. Nontronite did not dissolve to any measureable extent in experiments conducted with U(VI) under high pressure CO_2 conditions, indicating that both U(IV) and mild acidic conditions were necessary for nontronite dissolution. Under high pressure CO_2 conditions, structural Fe(II) dissolved to a greater extent over the 15 d reaction period.

Based on the different rates of uraninite oxidation in the presence and absence of elevated CO_2 concentrations, we can speculate on the mechanism of U(IV) oxidation by NAu-2 Fe(III). In another study, we used Mössbauer spectroscopy to characterize R-NAu-2 and found that Fe(II) was only in the octahedral sheet (Luan et al., 2014). Electron transfer from U(IV) to octahedral-Fe(III) could then occur either "directly" through edge sites (followed by electron hopping deeper into the clay structure) or "indirectly" through the basal plan [e.g., facilitated by tetrahedral Fe(III)]. Both of these mechanisms are likely operative but we are unable to determine which might be predominant. Unlike Fe(III) in nontronite, U(IV) in uraninite is not completely insoluble. Therefore, either soluble U(IV) or solid-phase U(IV) may be the form that donates electrons to octahedral-Fe(III). We contend that soluble U(IV) would be a more facile reductant as compared to solid-phase U(IV) because direct contact of uraninite with nontronite would not be required. Furthermore, the addition of CO_2 will increase the solubility of U(IV) and provides a simple explanation for why U(IV) was oxidized more quickly under these conditions.

4. Conclusion

Dissolution of unaltered nontronite was not measureable under high pressure CO_2 conditions. However, the reduction of structural Fe(III) in nontronite or reaction with strong acid (1.40 M H_3PO_4–0.50 M H_2SO_4) significantly increased the solubility of nontronite. The reduction of Fe(III)-bearing clay minerals can be promoted by the presence of redox-active contaminants such as uranium. Octahedral layers of NAu-2 dissolved more easily than tetrahedral layers and preferential dissolution occurred as: Mg > Fe ≈ Al > Si. R-NAu-2 Fe(II) appeared to be preferentially dissolved as compared to NAu-2 Fe(III). No redox reactions were observed between U(VI) and R-NAu-2 Fe(II). In comparison, redox reactions between uraninite(IV) and NAu-2 Fe(III) led to the dissolution of both minerals. In a GCS scenario, the addition of CO_2 to the sequestration strata or leaked into overlying strata would increase the solubility of both U(IV) and U(VI). CO_2-rich fluids could then facilitate the transport of U to the sequestration strata–cap rock interface or solubilize U from the cap rock. The co-occurrence of U(IV) and clay-Fe(III) in either strata plus the presence of elevated CO_2 concentrations will promote clay mineral dissolution. Redox reactions between contaminants and host minerals, therefore, represent another process where contaminant-mineral reactions can affect matrix permeability.

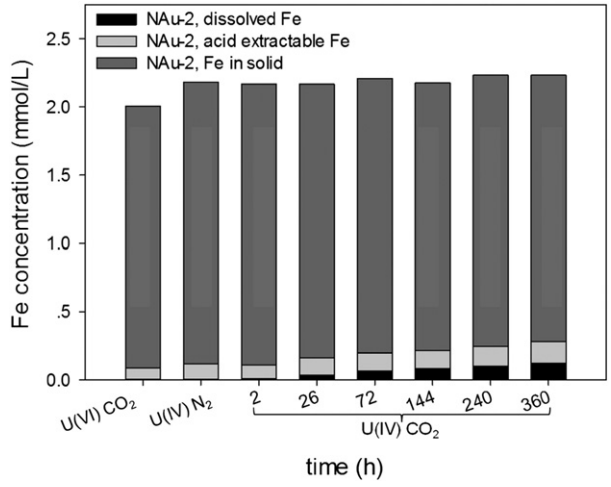

Fig. 5. Fe distribution in dissolved, 1.40 M H_3PO_4–0.50 M H_2SO_4 extractable, and solid forms. From left, first bar: high pressure CO_2 conditions (P_T = 9.66 bar, P_{CO_2} ≥ 8.66 bar CO_2) with U(VI); second bar: ambient pressure conditions (P_T = 1.0 bar, N_2:H_2 = 95:5%) with U(IV); all other bars represent reactions high pressure CO_2 conditions with U(IV) and increasing reaction time (# of hours). Experiments conducted with 0.5 g/L NAu-2 in 0.33 M Na_2SO_4.

Acknowledgments

This technical effort was performed in support of the US DOE National Energy Technology Laboratory's on-going research in CO_2-capture under the RES contract DE-FE-0004000. This project was funded by NETL through a support contract with URS Energy & Construction, Inc. The views and opinions of the authors expressed herein do not necessarily state or reflect those of the US government.

Appendix A. Supporting information

Illustration of sequential experimental methods and additional data are included in supporting information. Supplementary data to this article can be found online at http://dx.doi.org/10.1016/j.chemgeo.2014.06.009.

Appendix A. Supplementary data

Supplementary data to this article can be found online at http://dx.doi.org/10.1016/j.chemgeo.2014.06.009.

References

Bishop, M.E., Dong, H.L., Kukkadapu, R.K., Liu, C.X., Edelmann, R.E., 2011. Bioreduction of Fe-bearing clay minerals and their reactivity toward pertechnetate (Tc-99). Geochim. Cosmochim. Acta 75, 5229–5246.
Borch, T., Roche, N., Johnson, T.E., 2012. Determination of contaminant levels and remediation efficacy in groundwater at a former in situ recovery uranium mine. J. Environ. Monit. 14, 1814–1823.
Burgos, W.D., McDonough, J.T., Senko, J.M., Zhang, G., et al., 2008. Characterization of uraninite nanoparticles produced by *Shewanella oneidensis* MR-1. Geochim. Cosmochim. Acta 72, 4901–4915.
Canal, J., Delgado, J., Falcón, I., Yang, Q., Juncosa, R., Barrientos, V., 2013. Injection of CO_2-saturated water through a siliceous sandstone plug from the Hontomin test site (Spain): experiment and modeling. Environ. Sci. Technol. 47, 159–167.
Daneshfar, J., Hughes, R.G., Civan, F., 2009. Feasibility investigation and modeling analysis of CO_2 sequestration in arbuckle formation utilizing salt water disposal wells. J. Energy Res. Technol. 131 (023301-1-10).
Emberley, S., Hutcheon, I., Shevalier, M., Durocher, K., Gunter, W.D., Perkins, E.H., 2004. Geochemical monitoring of fluid–rock interaction and CO_2 storage at the Weyburn CO_2-injection enhanced oil recovery site, Saskatchewan, Canada. Energy 29, 1393–1401.
Gates, W.P., Slade, P.G., Manceau, A., Lanson, B., 2002. Site occupancies by iron in nontronites. Clay Clay Miner. 50 (2), 223–239.
Ginder-Vogel, M., Criddle, C.S., Fendorf, S., 2006. Thermodynamic constraints on the oxidation of biogenic UO2 by Fe(III) (hydr) oxides. Environ. Sci. Technol. 40, 3544–3550.
Ginder-Vogel, M., Stewart, B., Fendorf, S., 2010. Kinetic and mechanistic constraints on the oxidation of biogenic uraninite by ferrihydrite. Environ. Sci. Technol. 44, 163–169.
Griffith, C.A., Dzombak, D.A., Lowry, G.V., 2011. Physical and chemical characteristics of potential seal strata in regions considered for demonstrating geological saline CO_2 sequestration. Environ. Earth Sci. http://dx.doi.org/10.1007/s12665-011-0911-5.
IEAGHG, 2013. Interaction of CO2 Storage with Subsurface Resources (April).
Jaisi, D.P., Kukkadapu, R.K., Eberl, D.D., Dong, H.L., 2005. Control of Fe(III) site occupancy on the rate and extent of microbial reduction of Fe(III) in nontronite. Geochim. Cosmochim. Acta 69, 5429–5440.
Jaisi, D.P., Dong, H.L., Morton, J.P., 2008. Partitioning of Fe(II) in reduced nontronite (NAu-2) to reactive sites: reactivity in terms of Tc(VII) reduction. Clay Clay Miner. 56, 175–189.
Keating, E.H., Fessenden, J., Kanjorski, N., Koning, D.J., Pawar, R., 2010. The impact of CO_2 on shallow groundwater chemistry: observations at a natural analog site and implications for carbon sequestration. Environ. Earth Sci. 60, 521–536.
Keeling, J.L., Raven, M.D., Gates, W.P., 2000. Geology and characterization of two hydrothermal nontronites from weathered metamorphic rocks at the Uley Graphite Mine, South Australia. Clay Clay Miner. 48 (5), 537–548.

Kharaka, Y.K., Thordsen, J.J., Kakouros, E., Ambats, E., Herkelrath, W., et al., 2010. Changes in the chemistry of shallow groundwater related to the 2008 injection of CO_2 at the ZERT field site, Bozeman, Montana. Environ. Earth Sci. 60, 273–284.

Knauss, K.G., Johnson, J.W., Steefel, C.I., 2005. Evaluation of the impact of CO_2, co-contaminant gas, aqueous fluid and reservoir rock interactions on the geologic sequestration of CO_2. Chem. Geol. 217, 339–350.

Little, M.G., Jackson, R.B., 2010. Potential impacts of leakage from deep CO_2 geosequestration on overlying freshwater aquifers. Environ. Sci. Technol. 44, 9225–9232.

Luan, F.B., Burgos, W.D., 2012. Sequential extraction method for determination of Fe(II/III) and U(IV/VI) in suspensions of iron-bearing phyllosilicates and uranium. Environ. Sci. Technol. 46, 11995–12002.

Luan, F., Gorski, C.A., Burgos, D.B., 2014. Thermodynamic controls on the microbial reduction of iron-bearing nontronite and uranium. Environ. Sci. Technol. 48, 2750–2758.

Neumann, A., Hofstetter, T.B., Lussi, M., Cirpka, O.A., Petit, S., Schwarzenbach, R.P., 2008. Assessing the redox reactivity of structural iron in smectites using nitroaromatic compounds as kinetic probes. Environ. Sci. Technol. 42, 8381–8387.

Okada, K., Arimitsu, N., Karneshima, Y., Nakajima, A., MacKenzie, K.J.D., 2006. Solid acidity of 2: 1 type clay minerals activated by selective leaching. Appl. Clay Sci. 31, 185–193.

Olabode, A., Bentley, L., Radonjic, M., 2012. Shale caprock integrity under carbon sequestration conditions. AIP Conf. Proc. 1453, 347–352.

Osthaus, B., 1955. Kinetic studies on montmorillonites and nontronite by the acid-dissolution technique. Clay Clay Miner. 4, 301–321.

Pentrak, M., Madejova, J., Komadel, P., 2010. Effect of chemical composition and swelling on acid dissolution of 2: 1 clay minerals. Philos. Mag. 90, 2387–2397.

Ribeiro, F.R., Fabris, J.D., Kostka, J.E., Komadel, P., Stucki, J.W., 2009. Comparisons of structural iron reduction in smectites by bacteria and dithionite: II. a variable-temperature Mossbauer spectroscopic study of Garfield nontronite. Pure Appl. Chem. 81, 1499–1509.

Rimmele, G., Barlet-Gouedard, V., Renard, F., 2010. Evolution of the petrophysical and mineralogical properties of two reservoir rocks under thermodynamic conditions relevant for CO_2 geological storage at 3 km depth. Oil Gas Sci. Technol. 65, 565–580.

Rozalen, M.L., Huertas, F.J., Brady, P.V., Cama, J., et al., 2008. Experimental study of the effect of pH on the kinetics of montmorillonite dissolution at 25 degrees C. Geochim. Cosmochim. Acta 72, 4224–4253.

Sell, K., Enzmann, F., Kersten, M., Spangenberg, E., 2013. Microtomographic quantification of hydraulic clay mineral displacement effects during a CO_2 sequestration experiment with saline aquifer sandstone. Environ. Sci. Technol. 47, 198–204.

Senko, J.M., Kelly, S.D., Dohnalkova, A.C., McDonough, J.T., Kemner, K.M., Burgos, W.D., 2007. The effect of U(VI) bioreduction kinetics on subsequent reoxidation of biogenic U(IV). Geochim. Cosmochim. Acta 71, 4644–4654.

Shaw, S.A., Hendry, M.J., 2009. Geochemical and mineralogical impacts of H_2SO_4 on clays between pH 5.0 and −3.0. Appl. Geochem. 24, 333–345.

Steudel, A., Batenburg, L.F., Fischer, H.R., Weidler, P.G., Emmerich, K., 2009. Alteration of non-swelling clay minerals and magadiite by acid activation. Appl. Clay Sci. 44, 95–104.

Stucki, J.W., 2011. A review of the effects of iron redox cycles on smectite properties. Compt. Rendus Geosci. 343, 199–209.

Stucki, J.W., Golden, D.C., Roth, C., 1984. Effects of reduction and reoxidation of structural iron on the surface charge and dissolution of dioctahedral smectites. Clay Clay Miner. 32 (5), 350–356.

Ulrich, K.U., Ilton, E.S., Veeramani, H., Sharp, J.O., Bernier-Latmani, R., Schofield, E.J., Bargar, J.R., Giammar, D.E., 2009. Comparative dissolution kinetics of biogenic and chemogenic uraninite under oxidizing conditions in the presence of carbonate. Geochim. Cosmochim. Acta 73, 6065–6083.

White, C.M., Duane, H.S., Kenneth, L.J., Goodman, A.L., Sinisha, A.J., LaCount, R.B., 2005. Sequestration of carbon dioxide in coal with enhanced coalbed methane recovery: a review. Energy Fuel 19 (3), 659–724.

Xu, T.F., Apps, J.A., Pruess, K., 2004. Numerical simulation of CO_2 disposal by mineral trapping in deep aquifers. Appl. Geochem. 19, 917–936.

Xu, T., Apps, J.A., Pruess, K., Yamamoto, H., 2007. Numerical modeling of injection and mineral trapping of CO_2 with H_2S and SO_2 in a sandstone formation. Chem. Geol. 242, 319–346.

Zhang, G.X., Senko, J.M., Kelly, S.D., Tan, H., et al., 2009. Microbial reduction of iron(III)-rich nontronite and uranium(VI). Geochim. Cosmochim. Acta 73, 3523–3538.

Zheng, L.G., Apps, J.A., Zhang, Y.Q., Xu, T.F., Birkholzer, J.T., 2009. On mobilization of lead and arsenic in groundwater in response to CO_2 leakage from deep geological storage. Chem. Geol. 268, 281–297.

Zysset, M., Schindler, P.W., 1996. The proton promoted dissolution kinetics of K-montmorillonite. Geochim. Cosmochim. Acta 60, 921–931.